



PCCP

**A Crossed Molecular Beams and Computational Study on the Unusual Reactivity of Banana Bonds of Cyclopropane (c-C<sub>3</sub>H<sub>6</sub>; X1A1') through Insertion by Ground State Carbon Atoms (C(3Pj))**

Journal:	<i>Physical Chemistry Chemical Physics</i>
Manuscript ID	CP-ART-07-2022-003293.R1
Article Type:	Paper
Date Submitted by the Author:	23-Aug-2022
Complete List of Authors:	Galimova, Galiya; Florida International University, Chemistry and Biochemistry Mebel, Alexander; Florida International University, Chemistry and Biochemistry Goettl, Shane; University of Hawai'i at Manoa, Yang, Zhenghai; University of Hawai'i at Mānoa Kaiser, Ralf; University of Hawai'i at Mānoa

SCHOLARONE™  
Manuscripts

**A Crossed Molecular Beams and Computational Study on the Unusual  
Reactivity of Banana Bonds of Cyclopropane ( $c\text{-C}_3\text{H}_6$ ;  $X^1A_1'$ ) through  
Insertion by Ground State Carbon Atoms ( $C(^3P_j)$ )**

Galiya R. Galimova<sup>†</sup>, Alexander M. Mebel\*

*Department of Chemistry and Biochemistry, Florida International University, Miami, FL 33199,  
USA*

Corresponding Author Prof. Alexander M. Mebel: [mebela@fiu.edu](mailto:mebela@fiu.edu)

Shane J. Goettl<sup>†</sup>, Zhenghai Yang, Ralf I. Kaiser\*

*Department of Chemistry, University of Hawai'i at Mānoa, Honolulu, HI 96822, USA*

Corresponding Author Prof. Ralf I. Kaiser: [ralfk@hawaii.edu](mailto:ralfk@hawaii.edu)

<sup>†</sup>Both authors contributed equally to this work.

## ABSTRACT

The mechanism and chemical dynamics of the reaction of ground electronic state atomic carbon  $C(^3P_j)$  with cyclopropane  $c\text{-C}_3\text{H}_6$  ( $X^1A_1'$ ) have been explored by combining crossed molecular beams experiments with electronic structure calculations of the pertinent triplet  $C_4H_6$  potential energy surface and statistical computations of product branching ratios under single-collision conditions. The experimental findings suggest that the reaction proceeds via indirect scattering dynamics through triplet  $C_4H_6$  reaction intermediate(s) leading to  $C_4H_5$  product(s) plus atomic hydrogen via a tight exit transition state, with the overall reaction exoergicity evaluated as  $231 \pm 52 \text{ kJ mol}^{-1}$ . The calculations indicate that  $C(^3P_j)$  can easily insert into one of the three equivalent C-C 'banana' bonds of cyclopropane overcoming a low barrier of only  $2 \text{ kJ mol}^{-1}$  following the formation of a van der Waals reactant complex stabilized by  $15 \text{ kJ mol}^{-1}$ . The carbon atom insertion into one of the six C-H bonds is also feasible via a slightly higher barrier of  $5 \text{ kJ mol}^{-1}$ . These results highlight an unusual reactivity of cyclopropane's banana C-C bonds, which behave more like unsaturated C-C bonds with a  $\pi$ -character than saturated  $\sigma$  C-C bonds, which are known to be generally unreactive toward the ground electronic state atomic carbon such as in ethane ( $C_2H_6$ ). The statistical theory predicts the overall product branching ratios at the experimental collision energy as 50% for 1-butyn-4-yl, 33% for 1,3-butadien-2-yl,  $i\text{-C}_4H_5$ , and 11% for 1,3-butadien-1-yl,  $n\text{-C}_4H_5$ , with  $i\text{-C}_4H_5$  ( $230 \text{ kJ mol}^{-1}$  below the reactants) favored by the C-C insertion providing the best match with the experimentally observed reaction exoergicity. The  $C(^3P_j) + c\text{-C}_3H_6$  reaction is predicted to be a source of  $C_4H_5$  radicals under the conditions where its low entrance barriers can be overcome, such as in planetary atmospheres or in circumstellar envelopes but not in cold molecular clouds. Both  $i$ - and  $n\text{-C}_4H_5$  can further react with acetylene eventually producing the first aromatic ring and hence, the reaction of the atomic carbon with  $c\text{-C}_3H_6$  can be considered as an initial step toward the formation of benzene.

## 1. INTRODUCTION

Unsaturated and hydrogen-deficient resonance stabilized hydrocarbon free radicals (RSFRs) play an important role in the growth of polycyclic aromatic hydrocarbons (PAH), which in turn serve as precursors of soot and carbonaceous particles in various environments spanning from high-temperature combustion flames<sup>1-9</sup> and circumstellar envelopes to low-temperature planetary atmospheres and the interstellar medium (ISM).<sup>10-18</sup> The first stage of the PAH growth process is the formation of the first aromatic ring (benzene, C<sub>6</sub>H<sub>6</sub>; phenyl, C<sub>6</sub>H<sub>5</sub>) or two fused aromatic rings such as naphthalene (C<sub>10</sub>H<sub>8</sub>) from non-aromatic hydrocarbons, which is followed by their further enlargement through addition of extra six- or five-membered rings.<sup>3,19</sup> Both stages often proceed through the reactions involving RSFRs.<sup>20-25</sup> For example, the first aromatic ring is predominantly produced either via the odd C<sub>n</sub> route, i.e., through the recombination of two propargyl radicals, C<sub>3</sub>H<sub>3</sub>,<sup>26-30</sup> and the *i*-C<sub>5</sub>H<sub>3</sub> + CH<sub>3</sub> reaction,<sup>31</sup> or via the even C<sub>n</sub> route including the reactions like *n*-C<sub>4</sub>H<sub>3</sub> + C<sub>2</sub>H<sub>2</sub>, *n/i*-C<sub>4</sub>H<sub>5</sub> + C<sub>2</sub>H<sub>2</sub>,<sup>3</sup> and C<sub>4</sub>H<sub>6</sub> + C<sub>2</sub>H/C<sub>2</sub>.<sup>32,33</sup> The contribution of each of those reactions to the first aromatic formation depends on the conditions and the abundances of the radicals involved. But what is the original source of RSFRs themselves? In high temperature environments, they are produced by thermal decomposition of closed-shell hydrocarbons and accumulate due to their significantly higher stability and lower reactivity as compared to conventional free radical species. Alternatively, in low temperature conditions of ISM and planetary atmospheres photolysis may substitute the pyrolysis and also, RSFRs can be synthesized via bimolecular reactions of carbon atoms and small carbon clusters with unsaturated hydrocarbons.<sup>34,35</sup> Among them, the bimolecular reactions of ground-state carbon atoms C(<sup>3</sup>P<sub>j</sub>) with unsaturated hydrocarbons are of special importance because of the high abundance of atomic carbon in the Universe. Carbon atoms have been detected and identified in significant amounts via their 609 μm <sup>3</sup>P<sub>1</sub>-<sup>3</sup>P<sub>0</sub> transition in circumstellar envelopes of the carbon stars IRC + 10216 and α Orionis,<sup>36-39</sup> the proto planetary nebulae, such as CRL 618 and CRL 2688,<sup>40</sup> as well as in the diffuse cloud ζOph<sup>41</sup> and the dense cloud OMC-1.<sup>42</sup> Carbon atoms have been demonstrated both experimentally and theoretically to react with unsaturated hydrocarbons rapidly even at very low temperatures and to generate, through these reactions, a variety of RSFRs including C<sub>3</sub>H<sub>3</sub>,<sup>30,43</sup> C<sub>4</sub>H<sub>3</sub>,<sup>9,44,45</sup> and C<sub>4</sub>H<sub>5</sub>.<sup>34,35,46</sup> Theoretical calculations of the corresponding potential energy surfaces (PES) show that the reactions begin with the addition of C(<sup>3</sup>P<sub>j</sub>) to the π electronic density of an unsaturated hydrocarbon without an entrance barrier and then proceed to highly exoergic

products via intermediates and transition states residing lower in energy than the initial reactants. A representative example is the reaction of  $C(^3P_j)$  with the propylene molecule  $CH_2CHCH_3$  which was found, using crossed molecular beam and kinetic experiments and computational studies, to produce  $C_4H_5$  isomers 1-methylpropargyl, 3-methylpropargyl, and *i*- $C_4H_5$  (1,3-butadien-2-yl), via C-for-H replacement channels, as well as propargyl +  $CH_3$ .<sup>46-49</sup>

In a sharp contrast to unsaturated hydrocarbons, atomic carbon in its ground electronic state is nearly unreactive with saturated hydrocarbons. Only superthermal  $C(^3P_j)$  atoms generated by laser ablation of graphite and possessing an energy of 2 eV and higher could react with  $H_2$ , HCl, HBr,  $CH_3OH$ ,<sup>50,51</sup> and  $CH_4$ <sup>52</sup> according to experiments. The rate constant for the reaction of thermal  $C(^3P_j)$  with methane was evaluated to be less than  $5 \times 10^{-15} \text{ cm}^3 \text{ molecule}^{-1} \text{ s}^{-1}$  or even much lower at room temperature,<sup>53-55</sup> and no room or lower temperature reactivity is known for the ground state atomic carbon with ethane ( $C_2H_6$ ) or propane ( $C_3H_8$ ). This is due to the fact that the reaction barriers for insertion of  $C(^3P_j)$  into a single bond and for a direct H abstraction from a saturated molecule are high; for example, in the  $C(^3P_j) + CH_4$  reaction the computed barriers are 51 and 113  $\text{kJ mol}^{-1}$  for the insertion and abstraction channels, respectively.<sup>56</sup> An isomer of the unsaturated hydrocarbon propylene, cyclopropane  $c\text{-}C_3H_6$  ( $X^1A_1'$ ), is formally a saturated hydrocarbon but it is peculiar nevertheless.

Cyclopropane is a ring molecule with bent C-C single bonds known as ‘banana’ bonds. Cyclopropane cannot maintain conventional pure sigma bonds, since  $c\text{-}C_3H_6$  is a small cyclic molecule with three carbon atoms forming an equilateral triangle. The banana bonds in cyclopropane create interorbital angles of  $104^\circ$ , although the expected value for the triangular molecular shape is  $60^\circ$ . The C-C bonds in cyclopropane are weakened due to the bent bonds phenomenon, despite the fact that they are shorter than an ordinary C-C bond in a conventional alkane (1.51 Å versus 1.53 Å). Moreover, owing to some electron donation from the  $CH_2$  groups the C-C bonds in cyclopropane also acquire a partial  $\pi$  character. Therefore, the reactivity of  $c\text{-}C_3H_6$  is anticipated to be different from that of normal alkanes. This is indeed exemplified by the reaction mechanism of cyclopropane with  $O(^1D)$  which, according to crossed molecular beams experiments and PES calculations, can barrierlessly proceed by insertions of the atomic oxygen to both C-H and C-C bonds,<sup>57,58</sup> whereas the reactions of  $O(^1D)$  with small normal alkanes such as ethane and propane are dominated by the insertions only into C-H bonds.<sup>59,60</sup> But how the banana bonds in  $c\text{-}C_3H_6$  behave with respect to much less reactive ground electronic state atomic carbon

remains unknown. Is  $C(^3P_j)$  capable to readily attack the banana C-C bonds just like it does with double C=C and triple C $\equiv$ C bonds in unsaturated hydrocarbons or is it as unreactive as with normal alkanes?

The goal of the present work is to answer the above questions and to also assess the ability of the  $C(^3P_j)$  plus *c*-C<sub>3</sub>H<sub>6</sub> ( $X^1A_1'$ ) reaction to produce resonance stabilized C<sub>4</sub>H<sub>5</sub> radicals via a C-for-H replacement channel characteristic for the reactions of the ground-state atomic carbon with unsaturated hydrocarbons and thus to contribute to the PAH formation and growth by generating important RSFR precursors to the first aromatic ring. This goal is achieved by revealing the chemical dynamics of the elementary reaction of  $C(^3P_j)$  with *c*-C<sub>3</sub>H<sub>6</sub> ( $X^1A_1'$ ) under single collision conditions in crossed molecular beams. In combination with electronic structure and RRKM calculations, the results propose the prevalent formation of resonance stabilized isomers of the C<sub>4</sub>H<sub>5</sub> radicals via relatively low entrance barriers of a few kJ mol<sup>-1</sup> for unusual atomic carbon insertions into the C-C and C-H bonds making this reaction potentially important in planetary atmospheres and circumstellar envelopes of carbon stars, although not for cold molecular clouds.

## 2. EXPERIMENTAL

Reactions of atomic carbon ( $C, ^3P_j$ ) with cyclopropane (*c*-C<sub>3</sub>H<sub>6</sub>,  $X^1A_1'$ ,  $\geq 99\%$ , Sigma-Aldrich) were conducted under single collision conditions utilizing a universal crossed molecular beams machine.<sup>61-65</sup> Briefly, a pulsed supersonic beam of ground state carbon atoms was produced through a homemade laser ablation source exploiting a stepper motor (SP18074-3606) to rotate and helically translate a graphite rod<sup>66-68</sup> onto which the fourth harmonic output of a Nd:YAG laser (Quanta-Ray Pro 270, Spectra-Physics) operating at 30 Hz and 12 mJ per pulse was tightly focused to a spot size of less than 1.5 mm<sup>2</sup>. The ablated carbon atoms were seeded in helium (He, 99.9999 %, Airgas) at a backing pressure of 4 atm released by a Proch-Trickl<sup>69</sup> valve operating at 60 Hz with an amplitude of -400 V and opening times of 80  $\mu$ s. After entrainment of the ablated species, the beam passed through a skimmer and was velocity-selected by a four-slot chopper wheel. This resulted in a pulse characterized by a velocity,  $v_p$ , of  $2209 \pm 84$  m s<sup>-1</sup> and speed ratio,  $S$ , of  $3.1 \pm 0.2$ . The electronic states of atomic carbon have been determined previously; at the current velocity, carbon is only formed in its  $^3P_j$  ground state.<sup>66,70</sup> The carbon beam crossed perpendicularly with a pulsed supersonic beam of cyclopropane ( $v_p = 812 \pm 11$  m s<sup>-1</sup>,  $S = 11.6 \pm$

0.4) operated at 60 Hz with an amplitude of  $-400$  V and backing pressure of 550 Torr; this resulted in a collision energy,  $E_c$ , of  $25.8 \pm 1.9$  kJ mol $^{-1}$  and center-of-mass angle,  $\Theta_{CM}$ , of  $52.9 \pm 1.4^\circ$ . In addition to carbon atoms, laser ablation of the carbon rod results in dicarbon and tricarbon molecules.<sup>6,35,71,72</sup> Collision energies above 50 kJ mol $^{-1}$  are required to initiate reactions involving tricarbon molecules,<sup>73</sup> therefore tricarbon does not react with cyclopropane. The reaction of dicarbon with cyclopropane was explored at higher mass-to-charge ( $m/z$ ) ratios of 63, 64, and 65; however, no signal was found, indicating that dicarbon does not interfere with the title reaction under our experimental conditions.

Reactively scattered products were monitored by a triply differentially pumped universal detection system which is rotatable within the plane of the reactant beams. Upon entering the detector, neutral products are ionized by electron impact ionization at 80 eV at 2 mA before separation by a quadrupole mass filter (QC 150, Extrel) and amplification through a Daly type detector.<sup>74</sup> Up to  $8.7 \times 10^5$  time-of-flight (TOF) spectra were accumulated at angles between  $18 \leq \Theta \leq 66^\circ$  with respect to the carbon beam. The TOFs were integrated and normalized to extract the laboratory angular distribution. To obtain information on the reaction dynamics, the laboratory data were fit using a forward convolution routine.<sup>75,76</sup> This process transforms the data from the laboratory frame to the center-of-mass reference frame yielding the product translational energy,  $P(E_T)$ , and angular,  $T(\theta)$ , flux distribution in the center-of-mass (CM) reference frame. The CM functions define the product flux contour map which reveals the differential reactive cross section,  $I(u, \theta) \sim P(u) \times T(\theta)$ , as intensity with respect to the angle  $\theta$  and the CM velocity  $u$ .<sup>7</sup>

### 3. COMPUTATIONAL METHODS

The geometries of all species including reactants, products, intermediates and transition states involved in the C( $^3P_j$ ) plus c-C $_3$ H $_6$  ( $X^1A_1'$ ) reaction were optimized using the hybrid density functional B3LYP<sup>77,78</sup> and the 6-311G(d,p) basis set.<sup>79</sup> Vibrational frequencies and zero-point energy (ZPE) corrections were calculated at the same level of theory. All stationary points were characterized as local minima or transition states (TSs) on the PES using the computed frequencies. Optimized Cartesian coordinates and calculated vibrational frequencies for all structures involved in the reaction are given in Electronic Supplementary Information (ESI). The relative energies were refined using the explicitly correlated coupled clusters method<sup>80,81</sup> within the CCSD(T)-

F12/cc-pVQZ-f12//B3LYP/6-311G(d,p) + ZPE(B3LYP/6-311G(d,p)) scheme; the typical accuracy of this approach is within 4 kJ mol<sup>-1</sup> or better.<sup>82</sup> The Gaussian 09<sup>83</sup> and MOLPRO 2021<sup>84</sup> program packages were used for the ab initio calculations. The Rice–Ramsperger–Kassel–Marcus (RRKM) theory<sup>85</sup> was employed to calculate energy-dependent rate constants of individual unimolecular reaction steps following the formation of initial complexes. The rate constants were then used to compute product branching ratios under single-collision conditions using our in-house UNIMOL code.<sup>86</sup>

## 4. RESULTS

**4.1. Laboratory Frame.** The reaction of carbon (C, <sup>3</sup>P<sub>j</sub>) with cyclopropane (c-C<sub>3</sub>H<sub>6</sub>, X<sup>1</sup>A<sub>1</sub>') was probed for atomic and molecular hydrogen loss channels. TOF spectra were collected at  $\Theta_{\text{CM}}$  for  $m/z = 52$  (C<sub>4</sub>H<sub>4</sub><sup>+</sup>) and 53 (C<sub>4</sub>H<sub>5</sub><sup>+</sup>), which are superimposable after scaling (**Figure 1**). This indicates that only a single reaction channel is open in this elementary reaction; further, both masses arise from the same channel with signal at  $m/z = 52$  originating from dissociative electron impact ionization of the neutral product at 53 amu. Since the ion counts of the parent ion at  $m/z = 53$  (C<sub>4</sub>H<sub>5</sub><sup>+</sup>) were collected at a level of  $13 \pm 5\%$  compared to the fragment ion at  $m/z = 52$  (C<sub>4</sub>H<sub>4</sub><sup>+</sup>), the TOF spectra and laboratory angular distribution were acquired at the  $m/z$  of the highest signal-to-noise ratio, i.e. at  $m/z = 52$  (C<sub>4</sub>H<sub>4</sub><sup>+</sup>). The TOF spectra (**Figure 2B**) are very broad, typically ranging about 400  $\mu\text{s}$ . The laboratory angular distribution (**Figure 2A**) taken over the range of  $18 \leq \Theta \leq 66^\circ$  features a slight asymmetry about the center-of-mass angle of  $52.9 \pm 1.4^\circ$ , with greatest intensity about  $5^\circ$  lower than  $\Theta_{\text{CM}}$ . This finding suggests the reaction of carbon (C, <sup>3</sup>P<sub>j</sub>) with cyclopropane (c-C<sub>3</sub>H<sub>6</sub>, X<sup>1</sup>A<sub>1</sub>') proceeds via indirect scattering dynamics through C<sub>4</sub>H<sub>6</sub> reaction intermediate(s) leading to C<sub>4</sub>H<sub>5</sub> product(s) plus atomic hydrogen.

**4.2. Center-of-Mass Frame.** To reveal the chemical dynamics of the carbon plus cyclopropane reaction, the experimental data were transformed from the laboratory reference frame to the CM reference frame. The TOF spectra and laboratory angular distribution were fit with a single channel corresponding to the formation of a molecule of the molecular mass 53 amu (C<sub>4</sub>H<sub>5</sub>) and atomic hydrogen; **Figure 3** shows the best-fit functions. The maximum product translational energy release,  $E_{\text{max}}$ , is obtained from the product translational energy distribution,  $P(E_{\text{T}})$  (**Figure 3A**), with a derived value of  $257 \pm 50$  kJ mol<sup>-1</sup>. The conservation of energy dictates that the translational



energy can be derived from the collision energy, reaction energy, and internal energy of the products, given by  $E_T = E_c - \Delta_r G - E_i$ . For those reaction products born without internal excitation ( $E_i$ ), the reaction energy can be recovered with the formula  $\Delta_r G = E_c - E_{\max}$ , which denotes a reaction exoergicity for the title reaction of  $231 \pm 52 \text{ kJ mol}^{-1}$ . In addition, the  $P(E_T)$  exhibits a maximum at  $49 \text{ kJ mol}^{-1}$ , indicating a tight exit transition state and a large rearrangement of electron density from the decomposing reaction intermediate to  $\text{C}_4\text{H}_5$  and atomic hydrogen products.<sup>87</sup> Additional information on the reaction dynamics can be obtained by inspecting the CM angular flux distribution,  $T(\theta)$  (**Figure 3B**). First, flux intensity is shown along the entire angular range, reinforcing the implication of indirect scattering dynamics through  $\text{C}_4\text{H}_6$  intermediate(s). Second, the  $T(\theta)$  features a slight forward scattering with an intensity ratio  $I(0^\circ)/I(180^\circ)$  of about  $(1.5 \pm 0.2):1.0$ , which suggests the existence of at least one channel where complex formation takes place but the lifetime is too short to allow multiple rotations.<sup>88</sup> These findings are also reflected in the flux contour map (**Figure 3C**).

**4.3. Potential energy surface.** Our electronic structure calculations on the triplet  $\text{C}_4\text{H}_6$  PES predict that atomic carbon can add barrierlessly to a carbon-carbon bond in cyclopropane forming a van der Waals complex lying  $15 \text{ kJ mol}^{-1}$  below the energy of the  $\text{C}(^3\text{P}_j) + \text{c-C}_3\text{H}_6$  ( $\text{X}^1\text{A}_1'$ ) reactants (**Figure 4**). Next, the reaction continues by insertion of the attacking C atom into the C-C bond leading to a four-membered ring intermediate **i1** ( $305 \text{ kJ mol}^{-1}$  below the reactants) through a transition state (TS) residing  $2 \text{ kJ mol}^{-1}$  above the separated reactants. This result clearly indicates that the insertion of the ground state atomic carbon into a ‘banana’ C-C bond is a viable process. The **i1** intermediate can immediately lose a hydrogen atom from a  $\text{CH}_2$  group adjacent to the attacking carbon radical leading to the four-membered ring  $\text{C}_4\text{H}_5$  product **p5**,  $139 \text{ kJ mol}^{-1}$  lower in energy than the reactants through a TS lying  $131 \text{ kJ mol}^{-1}$  below the reactants. Also, the  $\text{CH}_2$  group opposite to the bare C atom in **i1** can split an H atom, with simultaneous formation of a new C-C bond across the ring, thus producing **p7** which has a bicyclic (rhombic) geometry made of two fused three-membered rings. However, this process is expected to be less competitive than the formation of **p5** + H because the corresponding TS resides only  $62 \text{ kJ mol}^{-1}$  below the reactants and the exothermicity of the **p7** + H products is  $68 \text{ kJ mol}^{-1}$ . In alternative to the H losses, **i1** can also isomerize. One possible isomerization pathway is the formation of isomer **i2** ( $293 \text{ kJ mol}^{-1}$  lower in energy than  $\text{C} + \text{C}_3\text{H}_6$ ) via 1,2-H migration from  $\text{CH}_2$  to the bare C atom through a TS

lying  $108 \text{ kJ mol}^{-1}$  below the reactants. The newly formed **i2** intermediate can also form the **p5** + H products losing a hydrogen atom from any of the two CH groups via a TS located  $123 \text{ kJ mol}^{-1}$  below the reactants' level. The barrier to form another rhombic bicyclic  $\text{C}_4\text{H}_5$  product **p6** by an H loss from **i2** is higher, with the corresponding TS at  $85 \text{ kJ mol}^{-1}$  relative to the reactants. In this case, a hydrogen atom is eliminated from one of the  $\text{CH}_2$  groups and this is accompanied by the C-C bond formation between the carbon atom that lost H and the opposite carbon. However, if a new C-C bond does not form upon the H loss from  $\text{CH}_2$  in **i2**, a more favorable four-membered ring product **p3**,  $-\text{CH}_2\text{CHCHCH}-$ , can be produced via a TS lying  $155 \text{ kJ mol}^{-1}$  below the reactants, with overall reaction exothermicity of  $225 \text{ kJ mol}^{-1}$ . The **i2** intermediate can also undergo a four-membered ring opening leading to the intermediate **i3** lying  $410 \text{ kJ mol}^{-1}$  lower in energy than  $\text{C} + \text{C}_3\text{H}_6$  via a TS residing  $203 \text{ kJ mol}^{-1}$  below the reactants. Next, **i3** can rearrange into **i4** ( $322 \text{ kJ mol}^{-1}$  lower in energy than the reactants) by a hydrogen migration between two CH groups neighboring one another via a TS at  $159 \text{ kJ mol}^{-1}$  below the reactants. Alternatively, **i4** can form directly by the four-membered ring opening of **i1** via a TS located  $183 \text{ kJ mol}^{-1}$  lower in energy than  $\text{C} + \text{C}_3\text{H}_6$ . The intermediate **i4** can isomerize to its slightly more favorable conformer **i5** ( $323 \text{ kJ mol}^{-1}$  below the reactants) by rotating the  $\text{C}=\text{CH}_2$  group around a single C-C bond via a tiny barrier of  $3 \text{ kJ mol}^{-1}$ . The isomer **i5** can dissociate to the products **p2**,  $\text{CH}_2\text{CHCCH}_2$  or  $i\text{-C}_4\text{H}_5$  ( $230 \text{ kJ mol}^{-1}$  below the energy of the  $\text{C}_3\text{H}_6 + \text{C}$ ), by losing one of the hydrogens from the central  $\text{CH}_2$  group via a TS located  $211 \text{ kJ mol}^{-1}$  lower than the reactants and **p4**,  $\text{CH}_2\text{CH}_2\text{CCH}$  ( $175 \text{ kJ mol}^{-1}$  below  $\text{C} + \text{C}_3\text{H}_6$ ), by eliminating an H atom from the  $\text{C}=\text{CH}_2$  group via a TS positioned  $158 \text{ kJ mol}^{-1}$  below the reactants. The central  $\text{CH}_2$  group in **i5** can shift a hydrogen to the central H-less carbon atom leading to the intermediate **i6** ( $413 \text{ kJ mol}^{-1}$  under the reactants' level), but the corresponding barrier (with TS lying  $141 \text{ kJ mol}^{-1}$  below the reactants) is significantly higher than those for the H losses from **i5**. Rotation around the central CH-CH bond in **i6** leads to its slightly more favorable conformer **i7** lying  $414 \text{ kJ mol}^{-1}$  below the reactants via a sizable barrier of  $60 \text{ kJ mol}^{-1}$ . **i7**, which appears to be the lowest energy minimum among all triplet  $\text{C}_4\text{H}_6$  isomers considered here, can also be formed from the isomer **i3** by  $90^\circ$ -twisting of one of the symmetrically equivalent  $\text{CH}_2$  groups around the corresponding CH- $\text{CH}_2$  bonds requiring a barrier of only  $1 \text{ kJ mol}^{-1}$ . This means that **i3** is likely to be only metastable with respect to its isomerization to **i7**. The isomer **i7** decomposes to the product **p2** by splitting a hydrogen atom from the CH group adjacent to the twisted  $\text{CH}_2$  group, rotated  $90^\circ$  relative to the molecular plain, via a TS positioned  $210 \text{ kJ}$

mol<sup>-1</sup> below the reactants. **i7** also can isomerize to the intermediate **i9** (393 kJ mol<sup>-1</sup> below the reactants' level) through hydrogen migration from the CH group adjacent to the twisted CH<sub>2</sub> group to this CH<sub>2</sub> via a TS located 205 kJ mol<sup>-1</sup> lower in energy than the reactants. The intermediate **i9** can also be obtained from **i4** via **i8** (386 kJ mol<sup>-1</sup> lower in energy than the reactants) through a pathway involving an H shift from the central CH<sub>2</sub> group to the adjacent terminal CH<sub>2</sub> moiety overcoming a barrier at a TS lying 188 kJ mol<sup>-1</sup> below the reactants, followed by another H migration from CH to bare C via a barrier at a TS located 186 kJ mol<sup>-1</sup> lower in energy than the reactants. The intermediate **i9** dissociates to **p2** by eliminating a hydrogen atom from the CH<sub>3</sub> group via a TS lying 224 kJ mol<sup>-1</sup> below the reactants. The intermediate **i8** can dissociate to the most exothermic propargyl C<sub>3</sub>H<sub>3</sub> + CH<sub>3</sub> products (**p1**, 270 kJ mol<sup>-1</sup> below the reactants) via the CH<sub>3</sub>-CH bond cleavage (TS lying 228 kJ mol<sup>-1</sup> lower in energy than the reactants). **i8** can also form **p2** through the hydrogen loss from the CH<sub>3</sub> group directly (TS at 210 kJ mol<sup>-1</sup> under the level of C + C<sub>3</sub>H<sub>6</sub>) and through the two-step mechanism where the H loss is preceded by the *cis-trans* conformational change of **i8** to **i10** via a significant rotational barrier of 93 kJ mol<sup>-1</sup>. The TS for the H loss from **i10** resides at 189 kJ mol<sup>-1</sup> below the reactants.

The additional reaction channels leading to products **p8-p10** are illustrated in **Figure 5**. The intermediate **i5** can form **i12** (309 kJ mol<sup>-1</sup> below the energy of the reactants) by transferring a hydrogen atom from the from the CH<sub>2</sub> group to the neighboring central carbon via a TS located 117 kJ mol<sup>-1</sup> below the reactants. **i12** can be also produced from **i1** via a metastable intermediate **i11** (100 kJ mol<sup>-1</sup> lower in energy than the reactants) through the pathway involving the four-membered ring opening by a C-CH<sub>2</sub> bond cleavage (TS positioned 88 kJ mol<sup>-1</sup> under the reactants' level) followed by the H migration from the central CH<sub>2</sub> group to the neighboring terminal bare carbon atom (TS lying 98 kJ mol<sup>-1</sup> below the reactants. The intermediate **i12** can undergo a change in conformation forming isomer **i14** (307 kJ mol<sup>-1</sup> below the reactants) via rotation around the CH-CH bond (TS located 293 kJ mol<sup>-1</sup> lower in energy than the reactants) and then **i14** can decompose to the **p10** products, triplet ethylene C<sub>2</sub>H<sub>4</sub> plus acetylene C<sub>2</sub>H<sub>2</sub>, lying 211 kJ mol<sup>-1</sup> below the reactants through the transition state lying 171 kJ mol<sup>-1</sup> lower in energy than C + C<sub>3</sub>H<sub>6</sub>. The isomers **i8** and **i10** can dissociate to the 1-methylpropargyl product **p9** (229 kJ mol<sup>-1</sup> below the reactants) by eliminating a hydrogen atom from the CH<sub>2</sub> group, with the corresponding TSs located 214 and 210 kJ mol<sup>-1</sup> under the reactants' level, respectively. The isomer **i9** can undergo a conformational

change to the intermediate **i13** (393 kJ mol<sup>-1</sup> below C + C<sub>3</sub>H<sub>6</sub>) via overcoming a modest barrier of 26 kJ mol<sup>-1</sup>. The 3-methylpropargyl product **p8** lying 240 kJ mol<sup>-1</sup> below the energy of the reactants can be formed through a hydrogen elimination from the central carbon atoms in the intermediates **i13** and **i10** with the corresponding TSs residing 222 and 217 kJ mol<sup>-1</sup> lower in energy than the reactants, respectively.

The atomic carbon can also insert into a C-H bond in cyclopropane forming **i15** lying 306 kJ mol<sup>-1</sup> below the energy of the reactants (**Figure 6**). In this case, the entrance barrier is calculated to be slightly higher than that for the insertion into the banana C-C bond, with the corresponding TS lying 5 kJ mol<sup>-1</sup> above the reactants. The loss of a hydrogen atom from the CH group in the three-membered ring of **i15** leads to the formation of products **p13** + H (121 kJ mol<sup>-1</sup> below the reactants). The same **p13** + H products can also be formed following isomerization of **i15** to **i16** (313 kJ mol<sup>-1</sup> lower in energy than the reactants) by H migration from CH in the ring to the out-of-ring CH moiety overcoming a barrier with a TS 103 kJ mol<sup>-1</sup> lower in energy than the reactants. The H loss TSs to produce **p13** + H from **i15** and **i16** respectively reside 109 and 112 kJ mol<sup>-1</sup> under the reactants' level. The isomer **i16** can also split an H atom from a ring CH<sub>2</sub> group leading to the product **p12** lying 162 kJ mol<sup>-1</sup> below the energy of the reactants via a TS located 103 kJ mol<sup>-1</sup> below C + C<sub>3</sub>H<sub>6</sub>. The intermediate **i16** can ring-open to CH<sub>2</sub>CH<sub>2</sub>CCH<sub>2</sub>, **i5** (323 kJ mol<sup>-1</sup> below the reactants) via a TS positioned 264 kJ mol<sup>-1</sup> lower in energy than the reactants, thus merging this section of the triplet C<sub>4</sub>H<sub>6</sub> PES accessed via the C insertion into a C-H bond with the part of the surface accessed by C insertion into a C-C bond (Figs. 4, 5). **i5** can rearrange to **i17**, CH<sub>2</sub>CH<sub>2</sub>CHCH, 307 kJ mol<sup>-1</sup> below the reactants via hydrogen migration from the -C-CH<sub>2</sub> group to the central bare carbon atom through a TS located 124 kJ mol<sup>-1</sup> below the reactants. The isomer **i17** can be formed more easily from the **i15** via ring opening with a TS lying 263 kJ mol<sup>-1</sup> under C + C<sub>3</sub>H<sub>6</sub>. Then, **i17** can decompose to the products **p4** (175 kJ mol<sup>-1</sup> lower in energy than the reactants) and **p11**, *n*-C<sub>4</sub>H<sub>5</sub>, 189 kcal mol<sup>-1</sup> below the reactants, through hydrogen eliminations from the central CH and CH<sub>2</sub> groups via TSs residing 154 and 164 kJ mol<sup>-1</sup> below the reactants' level, respectively. Clearly, the pathway C + C<sub>3</sub>H<sub>6</sub> → **i15** → **i17** → **p4/p11** + H is the most favorable one following the C-atom insertion into a C-H bond.

## 5. DISCUSSION AND CONCLUSIONS

We are now in position to combine the experimental and theoretical results and to unravel the mechanism of the  $C(^3P_j)$  plus  $c\text{-C}_3\text{H}_6$  reaction. The experiment provides the reaction exoergicity of  $231 \pm 52 \text{ kJ mol}^{-1}$  and points at an existence of a tight exit transition state connecting the decomposing triplet  $\text{C}_4\text{H}_6$  intermediate to  $\text{C}_4\text{H}_5$  plus H products. Several reaction products fall into this exoergicity range including **p2** (*i*- $\text{C}_4\text{H}_5$ ), **p3** (cyclobuten-3-yl), **p8** (3-methylpropargyl), **p9** (1-methylpropargyl), and **p11** (*n*- $\text{C}_4\text{H}_5$ ). All of these products are produced via tight transition states corresponding to distinct exit barriers in the range of 15-70  $\text{kJ mol}^{-1}$ . The other, less exoergic  $\text{C}_4\text{H}_5$  isomers can also be in principle produced as their signal can be buried under the slow portion of the experimental translational energy distribution. Looking at the PES accessed following the insertion of the attacking carbon atom into a C-C bond, one can see that the most energetically favorable reaction pathway leads to the formation of **p2**:  $C(^3P_j) + \text{C}_3\text{H}_6 \rightarrow \text{reactant complex} \rightarrow \mathbf{i1} \rightarrow \mathbf{i4} \rightarrow \mathbf{i5} \rightarrow \mathbf{p2} + \text{H}$ . The critical TS for this channel beginning from **i1** is the one for the four-membered ring opening in this intermediate leading to **i4** located 183  $\text{kJ mol}^{-1}$  under the reactants' level. The cyclobuten-3-yl product **p3** can be accessed by the H loss from **i2**, but the isomerization of **i1** is not competitive due the high barrier for **i1**  $\rightarrow$  **i2**. The methylpropargyl products can form via the following pathways:  $C(^3P_j) + \text{C}_3\text{H}_6 \rightarrow \text{reactant complex} \rightarrow \mathbf{i1} \rightarrow \mathbf{i4} \rightarrow \mathbf{i8} \rightarrow (\mathbf{i10} \rightarrow) \mathbf{p9} + \text{H}$  and  $C(^3P_j) + \text{C}_3\text{H}_6 \rightarrow \text{reactant complex} \rightarrow \mathbf{i1} \rightarrow \mathbf{i4} \rightarrow \mathbf{i8} \rightarrow \mathbf{i10} \rightarrow \mathbf{p8} + \text{H}$ , but these channels are anticipated to be less competitive as compared to the production of **p2**, since the isomerization of **i4** to **i5** exhibits a much lower barrier than that to **i8**. The *n*- $\text{C}_4\text{H}_5$  product **p11** is likely to be formed via a pathway initiated by C-insertion into a C-H bond in cyclopropane:  $C(^3P_j) + \text{C}_3\text{H}_6 \rightarrow \mathbf{i15} \rightarrow \mathbf{i17} \rightarrow \mathbf{p11} + \text{H}$ . Interestingly, the **p4** product  $\text{CH}_2\text{CH}_2\text{CCH}$  (1-butyn-4-yl) whose exoergicity is just outside of the experimentally determined range could be competitive since it can form both from **i5** and **i17**, which are expected to be the main decomposing intermediates in the C-C and C-H insertion channels, respectively.

Statistical RRKM calculations of the product branching ratios corroborate the qualitative picture described above (Table 1). If the unimolecular reaction of the triplet  $\text{C}_4\text{H}_6$  PES begins from intermediate **i1** following the C-C bond insertion, at the experimental collision energy, **p2** is predicted to be the main product (61%) followed by **p4** (27%), **p5** (7%), and propargyl +  $\text{CH}_3$  (**p1**, 3%). The minor products are formed either from the same decomposing complex **i5** (**p4**), or from the initial complex **i1** (**p5**), or via the intermediates **i4** and **i8** (**p1**). Considering **i15** as the initial

complex following the C-insertion into a C-H bond, **p4** and **p11** are predicted to be the main statistical products with the relative yields of 73% and 22%, respectively, with **p2** being a minor product at 4%. Here, both **p4** and **p11** are produced from the same decomposing complex **i17**, whereas **p2** is accessed from **i5**. Interestingly, the formation of **p4** from **i17** is favored by a looser TS despite the fact the H loss barrier toward **p11** is slightly lower than that leading to **p4**. From the energetic and molecular parameters of the entrance TSs for C-insertion into the C-C and C-H bonds, using RRKM rate constants to form **i1** and **i5** computed with an assumption that both pathways proceed from a common initial van der Waals complex, we can also evaluate the branching ratio in the entrance channel as 51%/49% where the slight energetic preference of the C-C insertion is nearly compensated by a factor of 2 higher reaction path degeneracy for the C-H insertion. Using the entrance channel branching ratio, the statistical theory finally predicts the overall relative yields to be: **p4** (1-butyne-4-yl) – 50%, **p2** (1,3-butadien-2-yl, *i*-C<sub>4</sub>H<sub>5</sub>) – 33%, and **p11** (1,3-butadien-1-yl, *n*-C<sub>4</sub>H<sub>5</sub>) – 11%, with minor contributions from **p5** (cyclobuten-1-yl), and **p1** (propargyl + CH<sub>3</sub>). Noteworthy is that the **p2** product matches the experimental reaction exoergicity best. This conclusion is also supported by a detailed inspection of two tight transition states leading to the **p2** product from intermediates **i5** and **i8** (Figure 7). The forward scattered center of mass angular distribution requires that the incorporated carbon atom and leaving hydrogen atom must be located on opposite sides of the rotational axis.<sup>89</sup> This requirement is fully supported in both transition states connecting to **p2** (Figure 7).

In our analysis so far, we considered only the triplet C<sub>4</sub>H<sub>6</sub> PES initially accessed by the C(<sup>3</sup>P<sub>j</sub>) reaction with *c*-C<sub>3</sub>H<sub>6</sub> (X<sup>1</sup>A<sub>1</sub>′). In the meantime, some intermediates on the most favorable reaction pathways, such as **i1**, **i4**, **i5**, **i8**, **i15**, and **i17** exhibit either carbene or biradical characters and therefore may have a close in energy singlet carbene or open-shell singlet states, respectively. In this case, intersystem crossing (ISC) from triplet to singlet PES could be in principle plausible. However, the present experimental results do not support any significant role of the singlet C<sub>4</sub>H<sub>6</sub> surface in the reaction. First, the C<sub>4</sub>H<sub>5</sub> products are formed via tight transition states with distinct exit barriers, whereas the decomposition of singlet C<sub>4</sub>H<sub>6</sub> species to C<sub>4</sub>H<sub>5</sub> + H should proceed without any exit barriers. Second, the most likely singlet intermediate to be produced after ISC is 1,3-butadiene, which could be formed, for example, from a singlet counterpart of **i1** via 1,2-H shift to the carbene site followed by facile ring opening in cyclobutene or by 1,2-H migration from CH<sub>2</sub> to the neighboring radical site in open-shell singlet **i4/i5**. The 1,3-butadiene molecule in this case

would have internal energy of  $657 \text{ kJ mol}^{-1}$ <sup>90</sup> plus the collision energy which is comparable with  $620 \text{ kJ mol}^{-1}$  acquired by hot 1,3-butadiene in its photodissociation process at 193 nm after internal conversion to the ground electronic state. Our previous statistical calculations of product branching ratios of photodissociation of 1,3-butadiene at this wavelength showed a significant yield of  $\text{H}_2$  loss  $\text{C}_4\text{H}_4$  products along with  $\text{C}_4\text{H}_5$ , with the predicted  $\text{H}/\text{H}_2$  loss branching ratio of 3.9/1.<sup>91</sup> In earlier crossed molecular beam experiments on the  $\text{C}(^3\text{P}_j) + \text{C}_2\text{H}_2$  reaction where ISC was found to play a role,  $\text{H}_2$  elimination products were unambiguously detected.<sup>92-97</sup> Here, however, no such products were observed which corroborates a minor (if any) contribution of the singlet PES.

Summarizing, the combined crossed molecular beams and computational study of the  $\text{C}(^3\text{P}_j)$  reaction with cyclopropane shows the formation of  $\text{C}_4\text{H}_5$  radicals together with atomic hydrogen via indirect scattering dynamics through triplet  $\text{C}_4\text{H}_6$  intermediates. The prevailing reaction products include the resonance stabilized *i*- $\text{C}_4\text{H}_5$  radical as well as its *n*- $\text{C}_4\text{H}_5$  and 1-butyn-4-yl isomers. The banana bond in cyclopropane reacts with the ground state atomic carbon more like an unsaturated C-C bond with a  $\pi$ -character than a saturated  $\sigma$  C-C bond. While the saturated C-C bonds are generally unreactive toward  $\text{C}(^3\text{P}_j)$ , here we observe facile insertions of the atomic carbon both into the C-C and C-H bonds which require overcoming rather low barriers of few  $\text{kJ mol}^{-1}$ . Therefore, the  $\text{C}(^3\text{P}_j) + \text{c-C}_3\text{H}_6$  reaction can serve as a source of  $\text{C}_4\text{H}_5$  radicals under the conditions where those low barriers can be overcome, such as in planetary atmospheres or in circumstellar envelopes. Since both *i*- and *n*- $\text{C}_4\text{H}_5$  can in principle react with acetylene eventually producing the first aromatic ring, the reaction of the atomic carbon with *c*- $\text{C}_3\text{H}_6$  can be considered as an initial step toward the formation of  $\text{C}_6\text{H}_6$ . However, on the contrary to the reactions of  $\text{C}(^3\text{P}_j)$  with unsaturated hydrocarbons, which proceed by barrierless additions of atomic carbon to  $\pi$  bonds,  $\text{C}(^3\text{P}_j) + \text{c-C}_3\text{H}_6$  exhibits small barriers both for the C-C and C-H insertion channels making this reaction too slow in the low-temperature conditions, such as in cold molecular clouds.

### Acknowledgements

This work was supported by the U.S. Department of Energy, Basic Energy Sciences, by Grants No. DE-FG02-04ER15570 to the Florida International University and No. DE-FG02-03ER15411 to the University of Hawaii at Manoa.

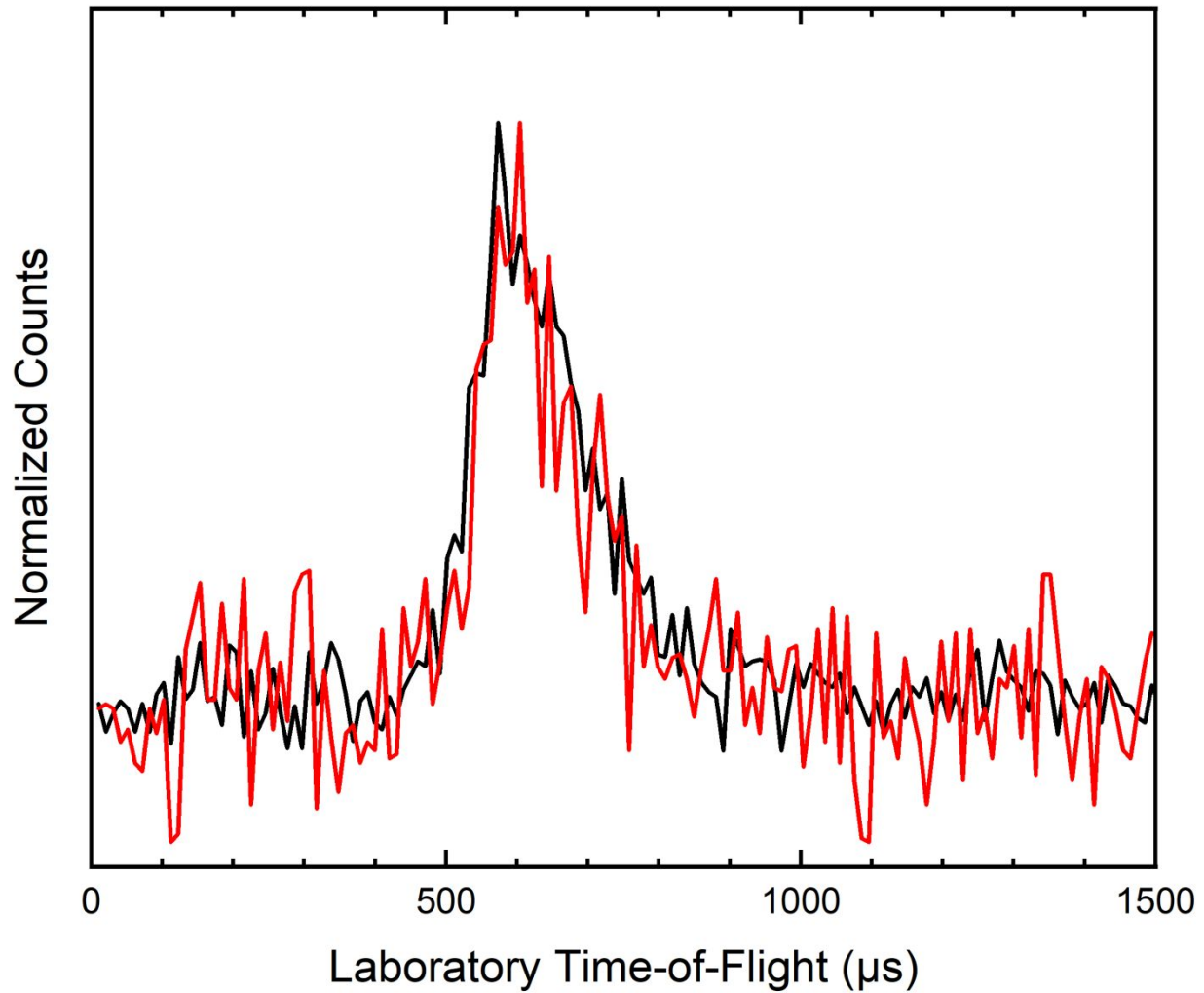


**Figure 1.** Normalized time-of-flight (TOF) spectra recorded at  $m/z = 52$  ( $C_4H_4^+$ , black) and 53 ( $C_4H_5^+$ , red) for the reaction of ground state atomic carbon ( $C, ^3P_j$ ) with cyclopropane ( $c-C_3H_6, X^1A_1'$ ).



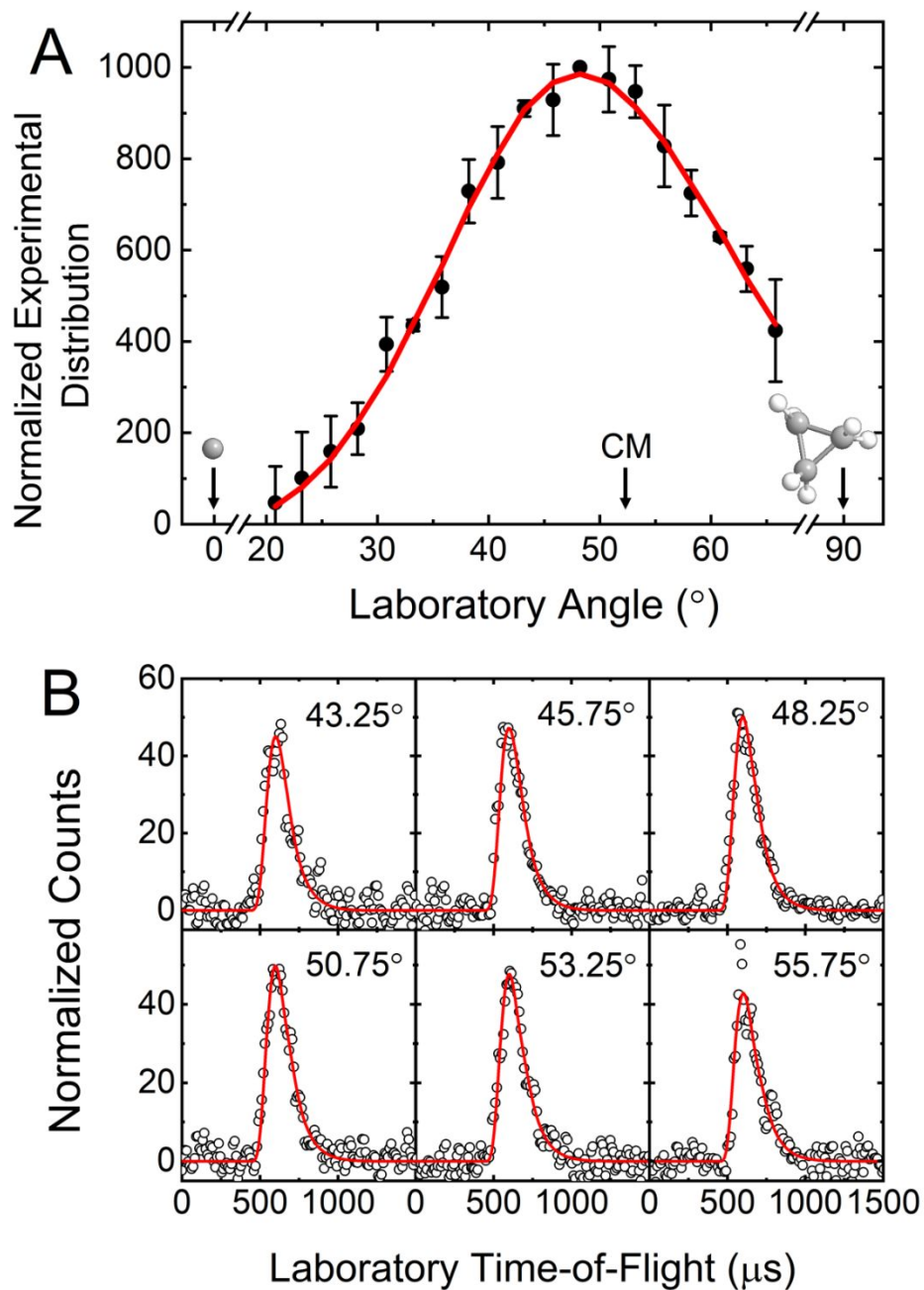


**Figure 2.** Laboratory angular distribution (A) and time-of-flight (TOF) spectra (B) recorded at mass-to-charge ( $m/z$ ) = 52 for the reaction of cyclopropane ( $c\text{-C}_3\text{H}_6$ ) with ground state atomic carbon. CM represents the center-of-mass angle, and  $0^\circ$  and  $90^\circ$  define the directions of the carbon and cyclopropane beams, respectively. The black circles depict the data, red lines the fits, and error bars the  $1\sigma$  standard deviation. Atoms are colored as follows: carbon (grey) and hydrogen (white).

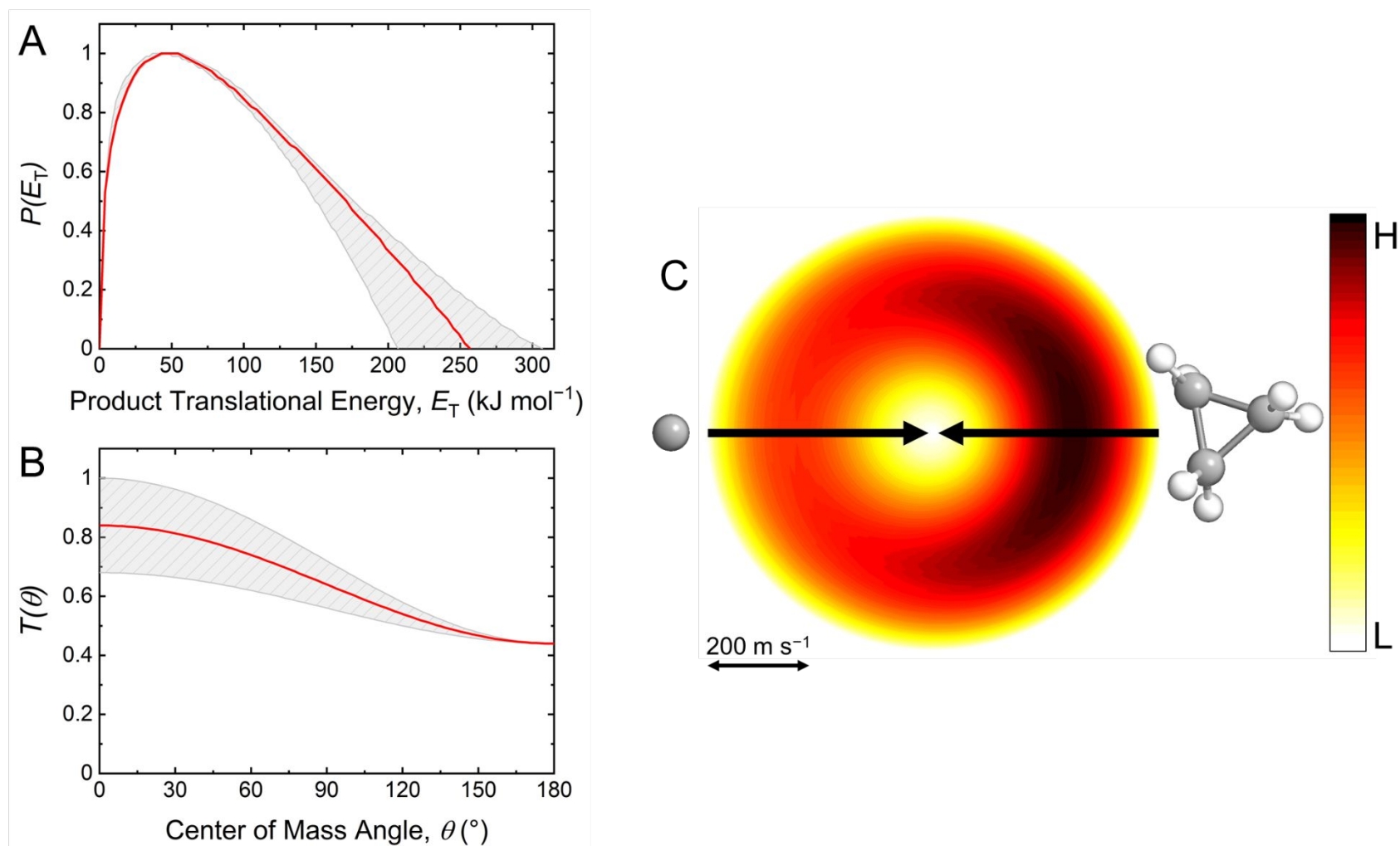


**Figure 3.** CM translational energy (A) and angular (B) flux distributions, as well as the associated flux contour map (C) leading to the formation of  $\text{C}_4\text{H}_5$  isomers plus atomic hydrogen in the reaction of ground state atomic carbon with cyclopropane ( $\text{c-C}_3\text{H}_6$ ). Red lines define the best-fit functions while shaded areas provide the error limits. The flux contour map represents the intensity of the reactively scattered products as a function of product velocity ( $u$ ) and scattering angle ( $\theta$ ), and the color bar indicates flux gradient from high (H) to low (L) intensity. Atoms are colored as follows: carbon (grey) and hydrogen (white).

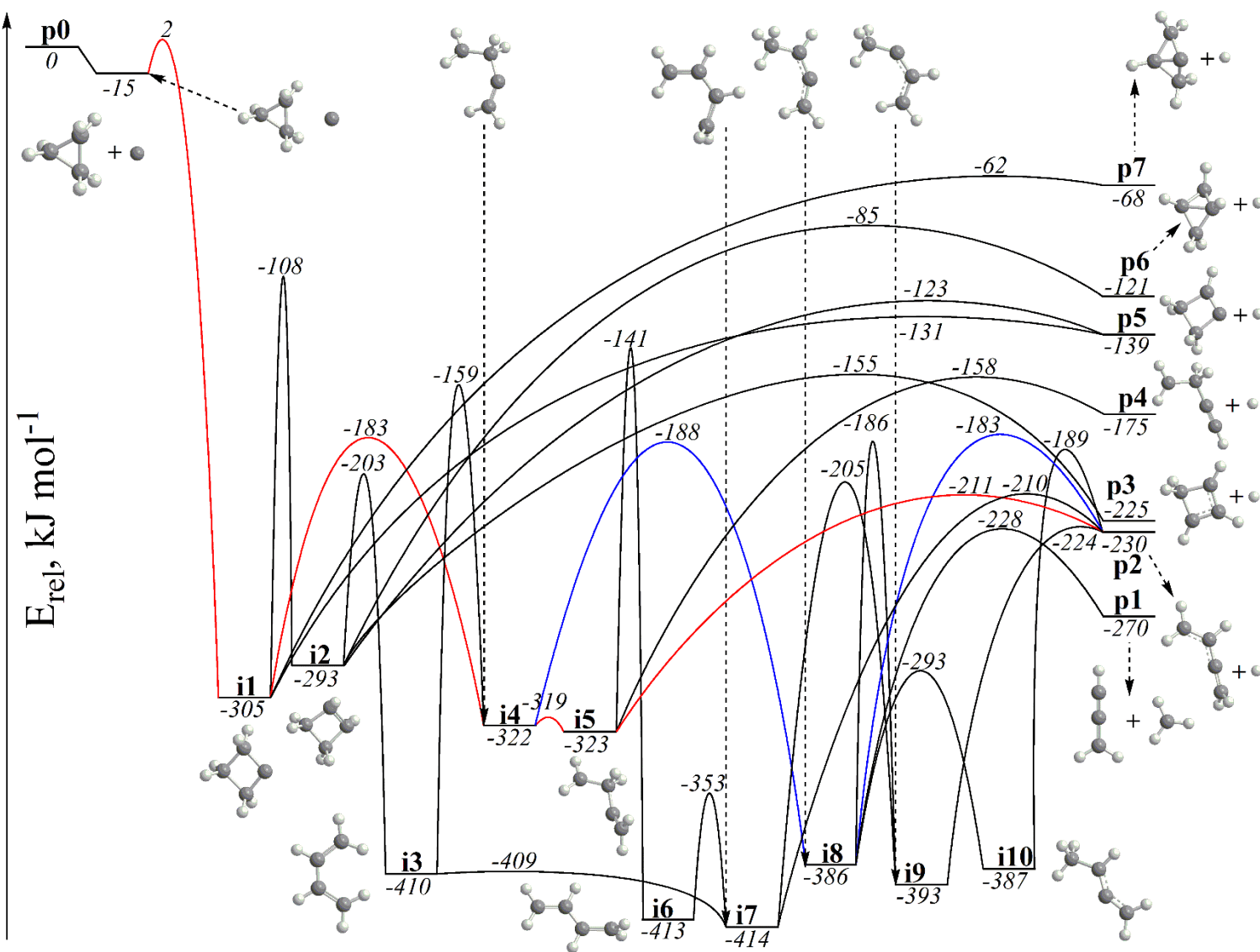


**Figure 4.** Portion of the  $C_4H_6$  PES leading to products **p1–p7** through intermediates **i1–i10**. The two preferable reaction pathways to **p2** are color coded in red and blue.

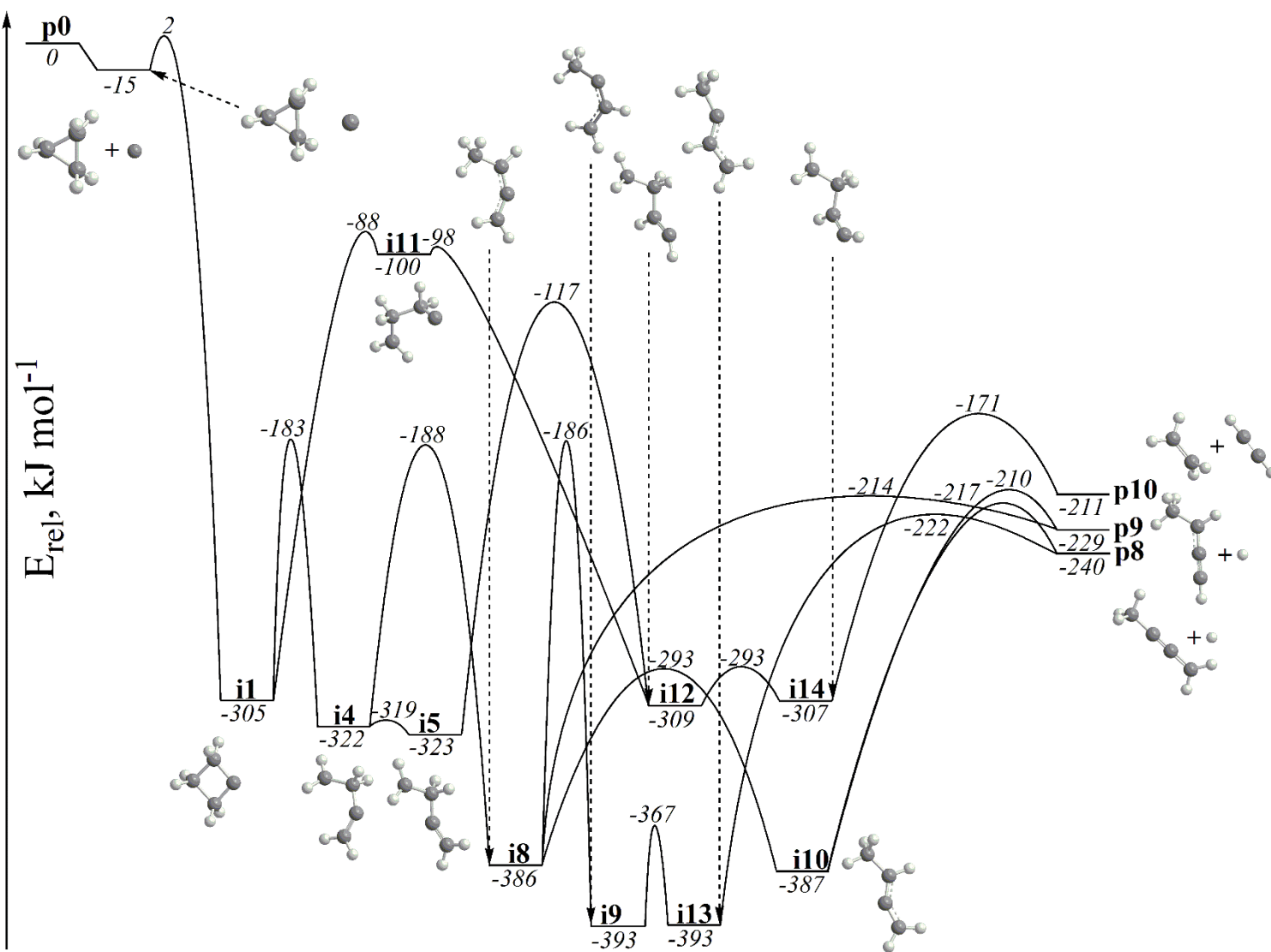


**Figure 5.** Portion of the  $C_4H_6$  PES leading to products **p8–p10** through intermediates **i1, i4–i5, and i8–i14**.

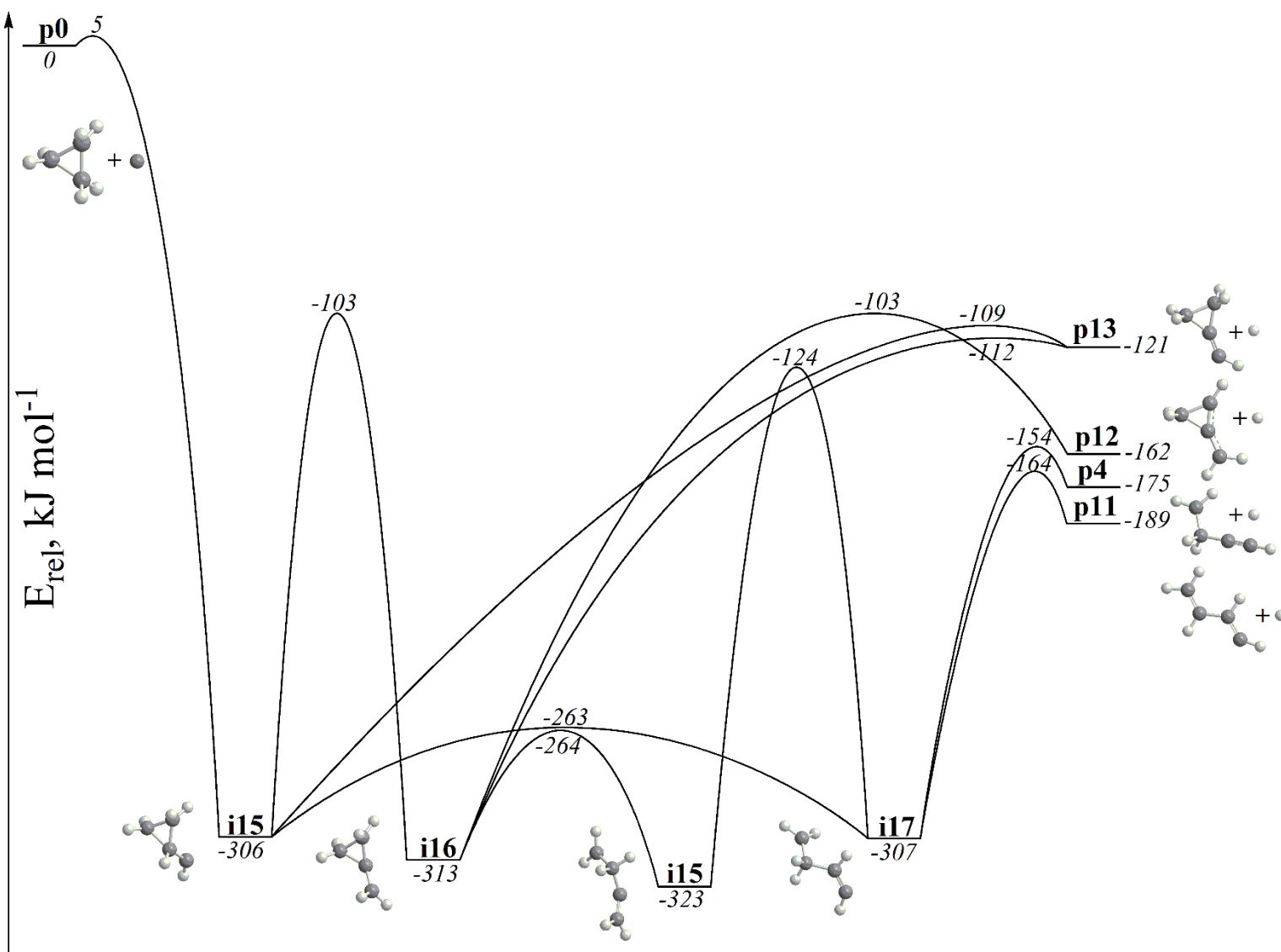


**Figure 6.** Portion of the  $C_4H_6$  PES leading to products **p4** and **p11–p13** through intermediates **i5** and **i15–i17**.

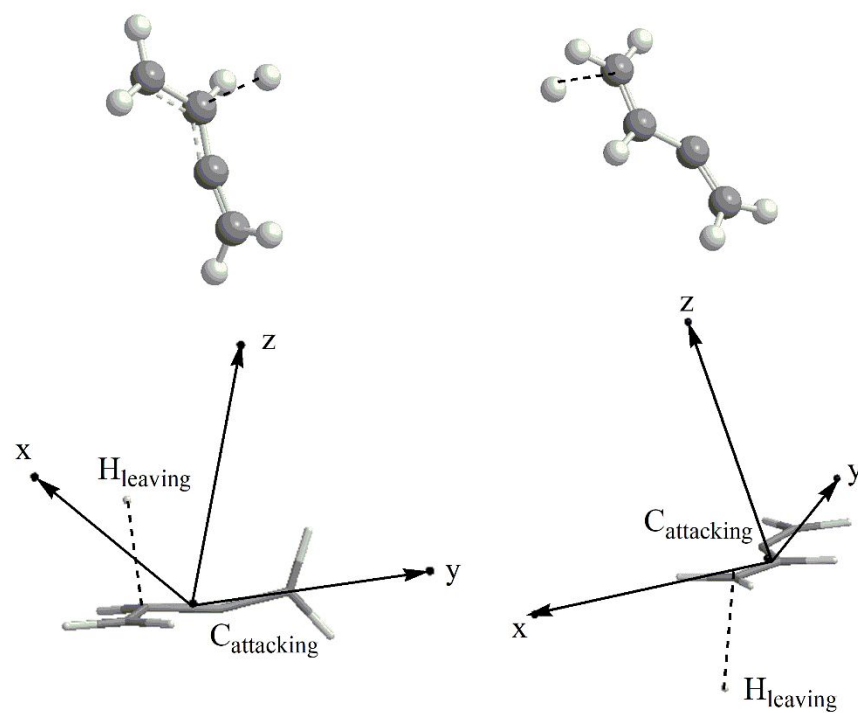


**Figure 7.** Geometry of the transition states and the three principle rotational axes connecting intermediates **i5** (left) and **i8** (right) to **p2** in the preferable reaction pathways shown in Figure 4.

**Table 1.** Statistical branching ratios (%) for the C + cyclopropane reaction at collision energies of 25.8 kJ mol<sup>-1</sup>.

Initial Intermediate	<b>i1</b> 100 %	<b>i15</b> 100 %	Total <sup>a</sup>
<b>p1</b>	3.00	0.19	1.63
<b>p2</b>	61.06	4.00	33.28
<b>p3</b>	0.06	0.00	0.03
<b>p4</b>	27.32	73.26	49.69
<b>p5</b>	7.07	0.00	3.63
<b>p6</b>	0.00	0.00	0.00
<b>p7</b>	0.05	0.00	0.03
<b>p8</b>	0.18	0.01	0.10
<b>p9</b>	0.67	0.04	0.36
<b>p10</b>	0.29	0.00	0.15
<b>p11</b>	0.27	22.46	11.08
<b>p12</b>	0.02	0.00	0.01
<b>p13</b>	0.01	0.04	0.02

<sup>a</sup>Calculated using the 51.3%/48.7% branching in the entrance channel between the insertion of C(<sup>3</sup>P<sub>j</sub>) into the C-C and C-H bonds, respectively.

## REFERENCES

- 1 H. Richter and J. B. Howard, *Prog. Energy Combust. Sci.*, 2000, **26**, 565-608.
- 2 M. J. Castaldi, N. M. Marinov, C. F. Melius, J. Hwang, S. M. Senkan, W. J. Pitz and C. K. Westbrook, *Symp. (Int.) Combust. Proc.*, 1996, **26**, 693-702.
- 3 M. Frenklach, *Phys. Chem. Chem. Phys.*, 2002, **4**, 2028-2037.
- 4 S. J. Goettl, C. He, D. Paul, A. A. Nikolayev, V. N. Azyazov, A. M. Mebel and R. I. Kaiser, *J. Phys. Chem. A*, 2022, **126**, 1889-1898.
- 5 A. M. Thomas, M. Lucas, T. Yang, R. I. Kaiser, L. Fuentes, D. Belisario-Lara and A. M. Mebel, *ChemPhysChem*, 2017, **18**, 1971-1976.
- 6 D. S. N. Parker, S. Maity, B. B. Dangi, R. I. Kaiser, A. Landera and A. M. Mebel, *Phys. Chem. Chem. Phys.*, 2014, **16**, 12150-12163.
- 7 R. I. Kaiser, *Chem. Rev.*, 2002, **102**, 1309-1358.
- 8 R. I. Kaiser, Y. T. Lee and A. G. Suits, *J. Chem. Phys.*, 1995, **103**, 10395-10398.
- 9 R. I. Kaiser, D. Stranges, Y. T. Lee and A. G. Suits, *Astrophys. J.*, 1997, **477**, 982-989.
- 10 Y. C. Minh, E. F. Dishoeck, *Astrochemistry – From Molecular Clouds to Planetary Systems*, ASP Publisher, San Francisco. 2000.
- 11 D. A. Williams, *Faraday Discuss.*, 1998, **109**, 1-14.
- 12 H. J. Fraser, M. R. S. McCoustra, D. A. Williams, *Astron. Geophys.*, 2002, **43**, 10-18.
- 13 R. I. Kaiser, C. Ochsenfeld, D. Stranges, M. Head-Gordon and Y. T. Lee, *Faraday Discuss.*, 1998, **109**, 183-204.
- 14 C. C. Chiong, O. Asvany, N. Balucani, Y. T. Lee and R. I. Kaiser, *Proceedings of the 8th Asia-Pacific Physics Conference*, 2001, 167-169.
- 15 M. Frenklach, D. W. Clary, W. C. Gardiner and S. E. Stein, *Symp. (Int.) Combust. [Proc.]*, 1984, **20**, 887-901.
- 16 C. He, K. Fujioka, A. A. Nikolayev, L. Zhao, S. Doddipatla, V. N. Azyazov, A. M. Mebel, R. Sun and R. I. Kaiser, *Phys. Chem. Chem. Phys.*, 2022, **24**, 578-593.
- 17 R. I. Kaiser, X. Gu, F. Zhang and P. Maksyutenko, *Phys. Chem. Chem. Phys.*, 2012, **14**, 575-588.
- 18 D. S. N. Parker, T. Yang, R. I. Kaiser, A. Landera and A. M. Mebel, *Chem. Phys. Lett.*, 2014, **595**, 230.
- 19 M. Frenklach, D. W. Clary, W. C. Gardiner, Jr. and S. E. Stein, *Proc. Combust. Inst.*, 1988, **21**, 1067-1076.
- 20 J. A. Miller, *Symp. (Int.) Combust. [Proc.]*, 1996, **26**, 461-480.
- 21 N. M. Marinov, W. J. Pitz, C. K. Westbrook, M. J. Castaldi and S. M. Senkan, *Combust. Sci. Technol.*, 1996, **116/117**, 211-287.
- 22 J. A. Miller and C. F. Melius, *Combust. Flame*, 1992, **91**, 21-39.
- 23 A. D'Anna, A. Violi, and A. D'Allesio, *Combust. Flame*, 2000, **121**, 418-429.
- 24 A. D'Anna and A. Violi, *Symp. (Int.) Combust. [Proc.]*, 1998, **27**, 425-433.
- 25 P. Lindstedt, *Symp. (Int.) Combust. [Proc.]*, 1998, **27**, 269-285.
- 26 J. A. Miller, *Faraday Discuss.*, 2001, **119**, 461-475.
- 27 J. A. Miller and S. J. Klippenstein, *J. Phys. Chem. A*, 2001, **105**, 7254-7266.
- 28 J. A. Miller and S. J. Klippenstein, *J. Phys. Chem. A*, 2003, **107**, 7783-7799.
- 29 L. Zhao, W. Lu, M. Ahmed, M. V. Zagidullin, V. N. Azyazov, A. N. Morozov, A. M. Mebel and R. I. Kaiser, *Science Adv.*, 2021, **7**, eabf0360.
- 30 R. I. Kaiser, Y. T. Lee and A. G. Suits, *J. Chem. Phys.*, 1996, **105**, 8705-8720.
- 31 A. M. Mebel, S. H. Lin, X. M. Yang and Y. T. Lee, *J. Phys. Chem. A*, 1997, **101**, 6781-6789.



- 32 B. M. Jones, F. Zhang, R. I. Kaiser, A. Jamal, A. M. Mebel, M. A. Cordiner and S. B. Charnley, *Proc. Nat. Acad. Sci.*, 2011, **108**, 452-457.
- 33 F. Zhang, B. Jones, P. Maksyutenko, R. I. Kaiser, C. Chin, V. V. Kislov and A. M. Mebel, *J. Am. Chem. Soc.*, 2010, **132**, 2672-2683.
- 34 R. I. Kaiser and A.M. Mebel, *Int. Rev. Phys. Chem.*, 2002, **21**, 307-356.
- 35 A. M. Mebel and R. I. Kaiser, *Int. Rev. Phys. Chem.*, 2015, **34**, 461-514.
- 36 J. Keene, K. Young, T. G. Phillips and T. H. Buttgenbach, *Astrophys. J.*, 1993, **415**, L131-L134.
- 37 W. E. C. J. Van Der Keen, P. J. Huggins and H. E. Matthews, *Astrophys. J.*, 1998, **505**, 749-755.
- 38 J. G. Ingalls, R. A. Chamberlin, T. M. Bania, J. M. Jackson, A. P. Lane and A. A. Stark, *Astrophys. J.*, 1997, **479**, 296-302.
- 39 C. D. Wilson, *Astrophys. J.*, 1997, **487**, L49-L52.
- 40 K. Young, *Astrophys. J.*, 1997, **488**, L157-L160.
- 41 U. J. Sofia, J. A. Cardelli, K. P. Guerin and D. M. Meyer, *Astrophys. J.*, 1997, **482**, L105-L108.
- 42 G. J. White and G. Sandell, *Astron. Astrophys.*, 1995, **299**, 179-192.
- 43 R. I. Kaiser, N. Balucani, D. O. Charkin and A. M. Mebel, *Chem. Phys. Lett.*, 2003, **382**, 112-119.
- 44 N. Balucani, A. M. Mebel, Y. T. Lee and R. I. Kaiser, *J. Phys. Chem. A*, 2001, **105**, 9813-9818.
- 45 R. I. Kaiser, D. Stranges, Y. T. Lee and A. G. Suits, *J. Chem. Phys.*, 1996, **105**, 8721-8733.
- 46 R. I. Kaiser, D. Stranges, H. M. Bevsek, Y. T. Lee and A. G. Suits, *J. Chem. Phys.*, 1997, **106**, 4945-4953.
- 47 R. I. Kaiser, T. L. Nguyen, T. N. Le and A. M. Mebel, *Astrophys. J.*, 2001, **561**, 858-863.
- 48 S. H. Lee, W. K. Chen, C. H. Chin and W. J. Huang, *J. Chem. Phys.*, 2013, **139**, 174-317.
- 49 J. C. Loison and A. Bergeat, *Phys. Chem. Chem. Phys.*, 2004, **6**, 5396-5401.
- 50 P. S. Skell, J. J. Havel and M. J. McGlinchey, *Acc. Chem. Res.*, 1973, **6**, 97-105.
- 51 M. R. Scholefield, S. Goyal, J. H. Choi and H. J. Reisler, *J. Phys. Chem.*, 1995, **99**, 14605-14613.
- 52 M. R. Scholefield, J. H. Choi, S. Goyal and H. J. Reisler, *Chem. Phys. Lett.*, 1998, **288**, 487-493.
- 53 F. F. Martinotti, M. J. Welch and A. P. Wolf, *Chem. Commun.*, 1968, 115-116.
- 54 W. Braun, A. M. Bass, D. D. Davis and J. D. Simmons, *Proc. R. Soc. London A*, 1969, **312**, 417-434.
- 55 D. Husain and L. J. Kirsch, *Trans. Faraday Soc.*, 1971, **67**, 2025-2035.
- 56 G.-S. Kim, T. L. Nguyen, A. M. Mebel, S. H. Lin and M. T. Nguyen, *J. Phys. Chem. A*, 2003, **107**, 1788-1796.
- 57 J. Shu, J. J. Lin, C. C. Wang, Y. T. Lee, X. Yang, T. L. Nguyen and A. M. Mebel. *J. Chem. Phys.*, 2001, **115**, 7-10.
- 58 C. C. Wang, J. Shu, J. J. Lin, Y. T. Lee, X. Yang, T. L. Nguyen and A. M. Mebel. *J. Chem. Phys.*, 2002, **116**, 8292-8299.
- 59 J. Shu, J. J. Lin, Y. T. Lee and X. Yang, *J. Chem. Phys.*, 2001, **114**, 4-7.
- 60 J. Shu, J. J. Lin, Y. T. Lee and X. Yang, *J. Am. Chem. Soc.*, 2001, **123**, 322-330.
- 61 X. Gu, Y. Guo, F. Zhang and R.I. Kaiser, *J. Phys. Chem. A*, 2007, **111**, 2980-2992.

- 62 Y. Guo, X. Gu, F. Zhang, M. S. Tang, B. J. Sun, A. H. H. Chang and R. I. Kaiser, *Phys. Chem. Chem. Phys.*, 2006, **8**, 5454-5461.
- 63 Y. Guo, X. Gu, F. Zhang, B. J. Sun, M. F. Tsai, A. H. H. Chang and R. I. Kaiser, *J. Phys. Chem. A.*, 2007, **111**, 3241-3247.
- 64 M. Lucas, A. M. Thomas, R. I. Kaiser, E. K. Bashkurov, V. N. Azyazov and A. M. Mebel, *J. Phys. Chem. A*, 2018, **122**, 3128-3139.
- 65 R. I. Kaiser, C. C. Chiong, O. Asvany, Y. T. Lee, F. Stahl, P. v. R. Schleyer and H. F. Schaefer III, *J. Chem. Phys.*, 2001, **114**, 3488.
- 66 R. I. Kaiser and A. G. Suits, *Rev. Sci. Instrum.*, 1995, **66**, 5405-5411.
- 67 X. Gu, Y. Guo, E. Kawamura and R. I. Kaiser, *J. Vac. Sci. Technol. A*, 2006, **24**, 505-511.
- 68 Y. Guo, X. Gu, E. Kawamura and R. I. Kaiser, *Rev. Sci. Instrum.*, 2006, **77**, 034701.
- 69 D. Proch and T. Trickl, *Rev. Sci. Instrum.*, 1989, **60**, 713-716.
- 70 R. I. Kaiser, A. M. Mebel and Y. T. Lee, *J. Chem. Phys.*, 2001, **114**, 231-239.
- 71 B. B. Dangi, D. S. N. Parker, R. I. Kaiser, D. Belisario-Lara and A. M. Mebel, *Chem. Phys. Lett.*, 2014, **607**, 92-99.
- 72 X. Gu, Y. Guo, A. M. Mebel, and R. I. Kaiser, *Chem. Phys. Lett.*, 2007, **449**, 44-52.
- 73 Y. Guo, X. Gu, F. Zhang, A. M. Mebel and R. I. Kaiser, *Phys. Chem. Chem. Phys.*, 2007, **9**, 1972-1979.
- 74 N. R. Daly, *Rev. Sci. Instrum.*, 1960, **31**, 264-267.
- 75 M. F. Vernon, *Molecular Beam Scattering*, PhD thesis, University of California at Berkeley, Berkeley, CA, 1983.
- 76 P. S. Weiss, *Reaction Dynamics of Electronically Excited Alkali Atoms with Simple Molecules*, PhD thesis, University of California at Berkeley, Berkeley, CA, 1986.
- 77 A. D. Becke, *J. Chem. Phys.*, 1992, **97**, 9173-9177.
- 78 C. Lee, W. Yang and R. G. Parr, *Phys. Rev. B*, 1988, **37**, 785-789.
- 79 R. Krishnan, M. Frisch and J. A. Pople, *J. Chem. Phys.*, 1988, **72**, 4244-4245.
- 80 T. B. Adler, G. Knizia and H.-J. Werner, *J. Chem. Phys.*, 2007, **127**, 221106.
- 81 G. Knizia, T. B. Adler and H.-J. Werner, *J. Chem. Phys.*, 2009, **130**, 054104.
- 82 J. Zhang and E. F. Valeev, *J. Chem. Theory Comput.*, 2012, **8**, 3175-3186.
- 83 M. J. Frisch, G. W. Trucks, H. B. Schlegel, G. E. Scuseria, M. A. Robb, J. R. Cheeseman, G. Scalmani, V. Barone, B. Mennucci and G. A. Petersson, *Gaussian 09 Revision A.1*, Gaussian, Inc., Wallingford CT, USA, 2009.
- 84 H. J. Werner, P. J. Knowles, R. Lindh, F. R. Manby, M. Schütz, P. Celani, T. Korona, G. Rauhut, R. D. Amos and A. Bernhardsson, *MOLPRO, version 2021.1, A Package of Ab Initio Programs*, University of Cardiff, Cardiff, UK, 2021, see <http://www.molpro.net>.
- 85 H. Eyring, S. H. Lin and S. M. Lin, *Basis Chemical Kinetics*, John Wiley & Sons, Ltd., New York, NY, 1980.
- 86 C. He, L. Zhao, A. M. Thomas, A. N. Morozov, A. M. Mebel and R. I. Kaiser, *J. Phys. Chem. A*, 2019, **123**, 5446-5462.
- 87 S. A. Safron, N. D. Weinstein, D. R. Herschbach and J. C. Tully, *Chem. Phys. Lett.*, 1972, **12**, 564-568.
- 88 W. B. Miller, S. A. Safron and D. R. Herschbach, *Discuss. Faraday Soc.*, 1967, **44**, 108-122.
- 89 R. I. Kaiser, C. Ochsenfeld, M. Head-Gordon, Y. T. Lee and A. G. Suits, *Science*, 1996, **274**, 1508-1511.
- 90 B. Ruscic, Active Thermochemical Tables, Version 1.122, available at <http://atct.anl.gov>.

- 91 H. Y. Lee, V. V. Kislov, S. H. Lin, A. M. Mebel and D. M. Neumark, *Chem. Eur. J.*, 2003, **9**, 726-740.
- 92 R. I. Kaiser, T. N. Le, T. L. Nguyen, A. M. Mebel, N. Balucani, Y. T. Lee, F. Stahl, P. v. R. Schleyer and H. F. Schaefer III, *Faraday Discuss.*, 2001, **119**, 51-66.
- 93 L. Cartechini, A. Bergeat, G. Capozza, P. Casavecchia, G. G. Volpi, W. D. Geppert, C. Naulin and M. Costes, *J. Chem. Phys.*, 2002, **116**, 5603-5611.
- 94 X. Gu, Y. Guo, F. Zhang and R. I. Kaiser, *J. Phys. Chem. A*, 2007, **111**, 2980-2992.
- 95 N. Balucani, J. Capozo, F. Leonori, E. Segoloni and P. Casavecchia, *Int. Rev. Phys. Chem.*, 2006, **25**, 109-163.
- 96 M. Costes, N. Daugey, C. Naulin, A. Bergeat, F. Leonori, E. Segoloni, R. Petrucci, N. Balucani and P. Casavecchia, *Faraday Discuss.*, 2006, **133**, 157-176.
- 97 A. Bergeat and J.-C. Loison, *Phys. Chem. Chem. Phys.*, 2001, **3**, 2038-2042.